Tornadoes in the Southeast United States: Investigating the Relationship between Intensity, Damage, and Terrain

MELANIE A. ZAMBRON*

National Weather Center Research Experiences for Undergraduates Program
Norman, Oklahoma

DAVID J. BODINE

Advanced Radar Research Center, University of Oklahoma
Norman, Oklahoma

ANTHONY E. REINHART

NOAA/OAR/National Severe Storms Laboratory
Norman, Oklahoma

ABSTRACT

With minimal past research, the impacts of terrain on tornadic-scale circulations remain unclear. This study utilizes data from individual NEXRAD radars, Multi-Radar Multi-Sensor (MRMS) products, damage surveys, and geological surveys to investigate relationships among tornado intensity, surface damage, and terrain height. Eight tornadoes, combined into six cases, from 2-3 March 2020 and 12-13 April 2020 are examined. Correlations are calculated for each case between six variables: rotational intensity (ΔV), maximum EF-scale rating, maximum MRMS Rotation Track value, damage width, velocity couplet width, and terrain height. Data for each variable are recorded at the 0.5° elevation scan time steps from the NEXRAD radars. Four of the six cases utilized additional low-level scans (SAILS) on the 0.5° tilt, but time gaps between updates limit available velocity data. The importance in distinguishing between tornado-level and mesocyclone-level winds in radar velocities based on range and beam height is discussed. Strong correlation coefficients are evident in higher-rated tornadoes between intensity variables, such as maximum EF rating and ΔV. Calculations with terrain indicate some moderate correlation with intensity variables and all weak correlations with damage variables. The moderate terrain correlations consist of only cases in which the radar scanned mesocyclone-level winds, so tornado-level winds examined by radar show only weak correlations with terrain.

1. Introduction

While the formation and impacts of tornadoes are well documented and understood, forecasting tornado occurrence still proves to be a challenge with relatively modest improvement in lead time and false alarm rate reduction (Brooks and Correia 2018). Variations in thermodynamic profiles and synoptic-scale features influence tornadogenesis in many ways, thus leaving each case unique and making forecasting difficult (Brown and Nowotarski 2020). Tornadoes are rated based on the extent of damage that they produce to structures with the Enhanced Fujita (EF) scale (WSEC 2006). However, when there are few structures or damage indicators along a tornado's path, determining the relationship between tornado intensity and

the EF-scale becomes problematic. In the southeastern United States, forests cover well over half of the land area, so the lack of structures increases the difficulty in assigning a damage rating to tornadoes in these areas (Oswalt et al. 2014; Godfrey and Peterson 2017).

Minimal research has been conducted involving the effects of complex terrain on tornadic-scale circulations. Suites of model simulations have shown that varying heights and shapes of topography influence the strength, structure, and path of a tornado, with the near-surface winds being most affected (Lewellen 2012; Satrio et al. 2020). Supercell storms also interact with terrain through upslope or downslope flow effects initiating modifications to thermodynamic variables, such as convective inhibition (CIN) and relative humidity (RH), as well as to hodograph shape (Markowski and Dotzek 2011). While the main circulation of a supercell or tornado can change with terrain variations, terrain also affects variables outside the

---

*Corresponding author address: Melanie Zambron, Department of Geography and Meteorology - Valparaiso University, 1700 Chapel Dr, Valparaiso, IN 46383
E-mail: melanie.zambron@valpo.edu

main damage track. Inflow winds have been shown to increase in speed when channeled in a valley, thus leading to damage features and downed trees outside the main track (Karstens et al. 2013).

Past studies have identified various radar signatures that are indicative of tornado presence. For instance, the tornadic debris signature (TDS) is a polarimetric signature created by lofted debris and is identified by low cross-correlation coefficient (ρ_{hv}) and differential reflectivity (Z_{DR}). Trends in TDS parameters have been shown to correlate well with damage surveys (Ryzhkov et al. 2005; Bodine et al. 2013). Additionally, increases in 0.5° peak rotational velocity (V_{rot}) and significant tornado parameter (STP) and decreases in circulation diameter have been shown to correlate with increased EF-scale damage (Smith et al. 2015; Thompson et al. 2017). It has also been noted that a greater threat for tornado formation exists when a tornadic vortex signature (TVS), or an area with high gate-to-gate shear, is easily spotted on radar (Thompson et al. 2017).

The purpose of this study is to further investigate the impacts of terrain on supercells and tornadoes and to explore the factors that contribute to differences in rotation signatures for tornadoes of similar strength. The study will utilize single-radar NEXRAD and Multi-Radar Multi-Sensor (MRMS) data (Smith et al. 2016). The MRMS system, developed at the National Severe Storms Laboratory (NSSL), is available for operational use as a tool to combine data from various sources to create blended products for severe weather, aviation, and hydrology purposes. Data sources for the MRMS system include individual NEXRADs, numerical models, satellites, and lightning strike data. Products are outputted approximately every two minutes on a 1-km grid covering the continental United States and southern Canada (Smith et al. 2016). The Warning Decision Support System – Integrated Information (WDSS-II) is one of the main programs used to create MRMS products and allows users to view these products on a display and overlay additional maps, such as for county or state boundaries (Lakshmanan et al. 2007).

2. Data and Methods

a. Single-Radar WSR-88D Data

The NEXRAD program's Weather Surveillance Radar-1988 Doppler (WSR-88D) were used in this study (Crum et al. 1998). The WSR-88D scans in a set volume coverage pattern (VCP). VCP 212 is a precipitation-mode volume coverage pattern programmed into the radar, typically selected when severe convection is located at a distance away from the radar. During severe convection, VCP 212 is recommended and allows for supplemental adaptive intra-volume low-level scans (SAILS) and multiple elevation scan option SAILS (MESO-SAILS) to occur. These adaptive scans allow for the 0.5° elevation scan
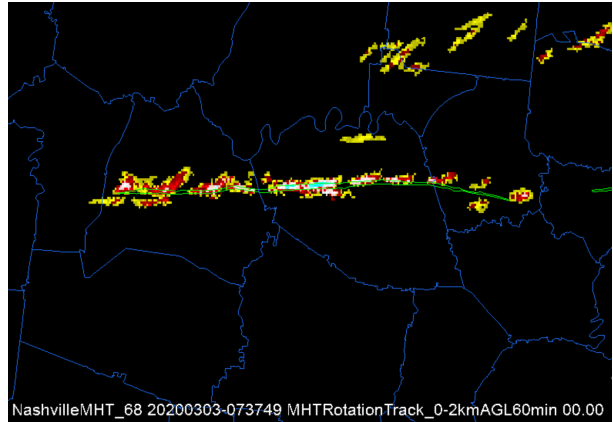

FIG. 1. WDSS-II display of 0-2 km Rotation Track product from the Nashville tornado, 3 March 2020. The damage track of the tornado is outlined in green.

to be updated every 90 s (Chrisman 2013a). The study used the lowest three elevation scans (0.5°, 0.9°, and 1.3°). The 0.5° scan updated approximately every two minutes, whereas the 0.9° and 1.3° scans updated approximately every six minutes.

To quantify rotational strength, the maximum inbound (negative) and outbound (positive) velocities at each time step and each elevation scan were recorded. Adding the absolute value of these two velocities together produced Delta V (ΔV), a value calculated to estimate rotational intensity at each time step (Brown et al. 1978; Mitchell et al. 1998). The study examined ground-relative velocities, so at some times the velocity couplet signature consisted of only outbound values due to the rapid translation of the tornado, with the southern part (relative to the tornado track) indicating stronger outbound flow. In these cases, the smaller outbound value was subtracted from the higher outbound value to determine ΔV.

b. MRMS Rotation Track

MRMS Rotation Tracks indicate the highest azimuthal shear (AzShear) that occurred every two minutes (Miller et al. 2013; Mahalik et al. 2019). This product was then accumulated over several times ranging from 30 minutes to several hours resulting in tracks of high AzShear. The low level (0-2 km) Rotation Track product from the MRMS system (Fig. 1) was recorded at the same times as the 0.5° Doppler velocities.

In order to make a reasonable comparison of this product to ΔV, Rotation Track values were recorded by comparing the product to the location of the velocity couplet at each single-radar 0.5°-time step. The maximum Rotation Track value within a few gates of the velocity couplet center was then extracted. The WDSS-II display allowed for simple comparison between the two different products to determine the maximum values.

c. Damage Data

Damage surveys of the 2-3 March 2020 tornadoes were performed by the Nashville, TN WFO, and damage surveys of the 12-13 April 2020 tornadoes were performed by the Jackson, MS WFO, the Birmingham, AL WFO, and the Morristown, TN WFO. The along-track damage survey was acquired from the NWS Damage Assessment Toolkit. Contours of maximum EF-scale rating from damage survey data were overlaid with the velocity and Rotation Track data and examined to calculate the width of the damage path. At each 0.5°-time step, the maximum EF-scale rating that aligned with the velocity couplet center was recorded. Additionally, at the same time steps and locations, the range and azimuth of the top and bottom points of the EF-0 contour were recorded in order to determine the width of the damage track. For the Bassfield tornado, the EF-0 contour data was inaccessible in the Damage Assessment toolkit, so the EF-1 contour was used instead. The EF-0 damage area is not much wider than the EF-1 damage, so the EF-1 damage width provides a reasonable estimation. We calculated x- and y-coordinates from the range and azimuth values by using the following equations:

$$x = R\sin\theta \qquad (1)$$

$$y = R\cos\theta \qquad (2)$$

where R represents the range from the radar and θ represents the azimuth around the radar. For the 12-13 April tornadoes, the tornadoes travelled roughly towards the northeast, so the distance formula (3) was utilized to determine the width of the track. Since the 2-3 March tornadoes traveled nearly eastward, the y-coordinate of the top point was subtracted from the y-coordinate of the bottom point to determine the width of the track in the north-south direction.

$$d = \sqrt{(x_2 - x_1)^2 + (y_2 - y_1)^2} \qquad (3)$$

d. Terrain Data

Terrain height data was obtained from the United States Geological Survey (USGS) The National Map (TNM) Elevation website. The site allows users to input latitude and longitude coordinates and outputs the terrain height at the location. Coordinate values were determined by the location of the center of the velocity couplet along the tornado tracks at the 0.5°-time steps.

e. Quality Control and Data Issues

Data for maximum and minimum velocities and Rotation Tracks were both recorded by hand. Suspect data points that seemed unreasonable and were likely the result of clutter or inaccurate velocity aliasing were removed. Excluded values included single gates with velocities significantly different from surrounding gates (e.g., with a difference greater than $20 - 30$ m s^{-1}) and areas with questionable velocity gradients. Additionally, several time steps showed a weaker velocity couplet, so horizontal continuity between adjacent time steps and vertical continuity between elevation scans were examined to determine the couplet's location. The velocity dealiasing algorithm for the Nashville NEXRAD radar (KOHX) failed in at least one time step, so to mitigate any other potential errors, the rest of the dealiased values were hand-calculated and compared with the algorithm output. To dealias by hand, the Nyquist velocity was multiplied by two and added to (subtracted from) the aliased inbound (outbound) velocity value. For KOHX, the Nyquist velocity was 33.3 m s^{-1}.

The Rotation Track values required little additional QC since they incorporated numerous data points from MRMS's QCed dealiased velocity field. However, the values were recorded at the center location of the single-radar velocity couplet. With some less-defined and broader couplets at some time steps, the center location was not always clearly defined. Thus, the maximum values were selected from within a few gates around the determined center of the couplet to account for potential error in the location of the couplet.

The Nashville tornado lasted about 63 minutes; however, the first half of the tornado's track is not clearly defined on KOHX due to clutter and sidelobe contamination effects on the radar signal (e.g., from the city of Nashville). The extensive amount of clutter and sidelobe contamination present due to the buildings and improper dealiasing make distinguishing a clear velocity couplet difficult for the first half of the tornado. Thus, we decided to only analyze the second half of the Nashville tornado track where the velocity data have fewer artifacts, from approximately 07:00 UTC (1:00 AM CST) to the tornado's demise 35 minutes later.

3. Event Overview

a. 2-3 March 2020

The late-night hours of March 2 to the early morning hours of March 3 brought severe storms capable of producing tornadoes to the southeastern United States. Supercells tracked through states such as Missouri, Kentucky, Alabama, and Tennessee. In Tennessee alone, a total of ten tornadoes (Fig. 2) touched down and travelled from the west side of the state to the east with fast storm motion speeds, ranging from 22 to 31 m s^{-1} (43 to 60 kts). Two tornadoes in Tennessee were examined from this event, one which passed through Nashville, TN and the other through Cookeville, TN. While several of the tornadoes produced minimal damage and received lower EF-scale ratings, the Nashville and Cookeville tornadoes received ratings of EF-3 and EF-4, respectively. The Nashville tornado travelled a path length of 96.77 km from 06:32 to 07:35 UTC (12:32 AM to 1:35 AM CST), injuring 220
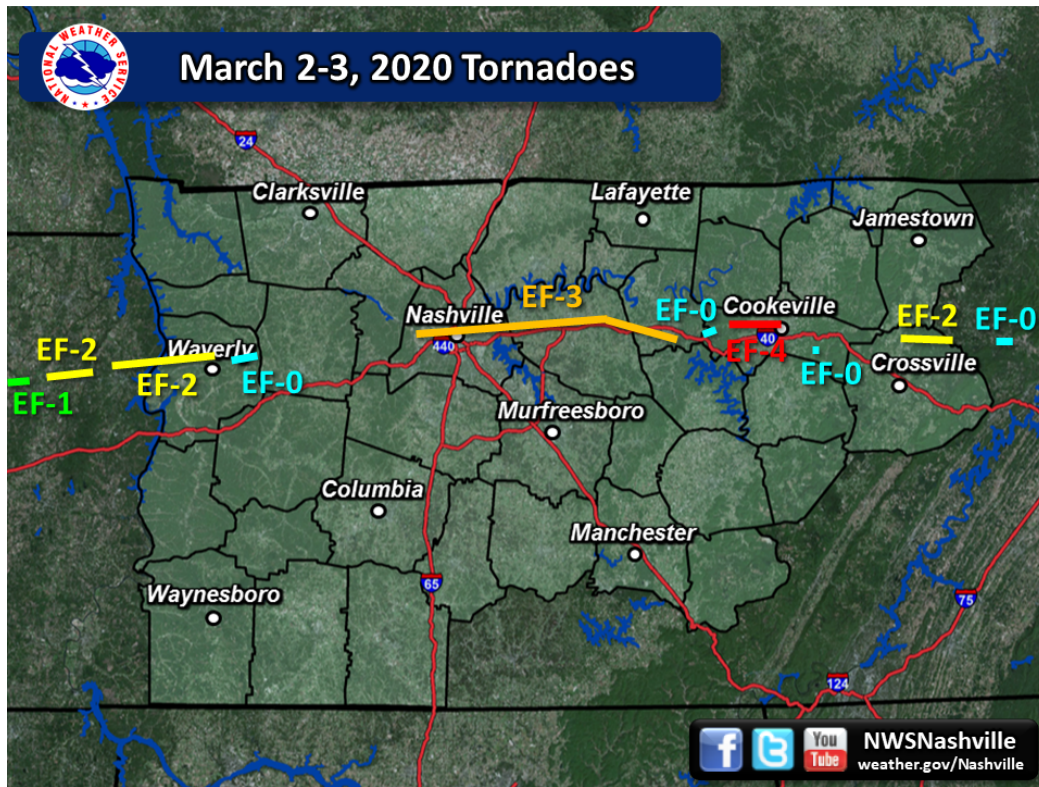
FIG. 2. Tornado tracks from the 2-3 March 2020 event in Tennessee. The 10 tornadoes are shown with the Nashville tornado in orange and the Cookeville tornado in red. Credit: NWS Nashville

and killing 5 people. The Cookeville tornado travelled a path length of 13.5 km from 07:48 to 07:56 UTC (1:48 AM to 1:56 AM CST), injuring 87 and killing 19 people.

Relative to KOHX, the Nashville tornado tracked from the southwest side to the southeast side, moving eastward with a slight southward curve near the track end. The Cookeville tornado, which touched down only thirteen minutes after the Nashville tornado dissipated, continued the eastward track. The radar viewing angle and range changed considerably between the two tornado events. Distance from KOHX ranged from 7 to 68 km for the Nashville tornado and from 83 to 94 km for the Cookeville tornado. Azimuth (direction) around KOHX spanned from 261° (WSW) to 93° (ESE) for the Nashville tornado and from 96° (ESE) to 93° (ESE) for the Cookeville tornado. The radar beam scanned the tornado level for the Nashville tornado, with heights between 0.3 km to 0.96 km AGL, and the mesocyclone level for the Cookeville tornado, with heights between 1.3 km to 1.56 km AGL. The maximum Rotation Track values for the Nashville and Cookeville tornadoes were 0.030 s^{-1} and 0.023 s^{-1}, respectively.

b. 12-13 April 2020

For the 24 hour period starting 12:00 UTC (7:00 AM CDT) on Easter Sunday to the following Monday, the NWS issued 141 tornado warnings throughout the southeastern United States. A total of 140 tornadoes touched down, with storms and damaging winds spanning from Texas to Maryland. Several long-track tornadoes occurred during this event in states such as Mississippi, Georgia, and South Carolina. Two EF-4, the Walthall and Bassfield tornadoes, and one EF-3, the Oak Vale tornado, passed through Mississippi (Fig. 3). The Walthall tornado travelled a path length of 34.11 km from 20:39 to 21:05 UTC (3:39 PM to 4:05 PM CDT), injuring 3 and killing 4 people. The Bassfield tornado travelled a path length of 109.07 km from 21:12 to 22:28 UTC (4:12 PM to 5:28 PM CDT), injuring 95 and killing 8 people. The Oak Vale tornado travelled a path length of 135.35 km from 21:36 to 23:07 UTC (4:36 PM to 6:07 PM CDT), with 2 injuries and no deaths. The Walthall and Bassfield tornadoes will be analyzed together and plotted on the same figures due to the same rating, short time period between tornadoes, and similar statistical characteristics.

The long-track Oak Vale tornado was only several miles north of the Bassfield tornado, which is one of Mississippi's widest tornadoes on record with a peak width of 3.62 km. Distance from the Jackson, MS NEXRAD radar (KDGX) for the two EF-4 tornadoes and the Oak Vale tornado ranged from 86 km to 110 km and from 76 km to 101 km, respectively. Azimuth (direction) around KDGX spanned from 99° (ESE) to 189° (SSW) for the two EF-4 tornadoes and the Oak Vale tornado. The radar beam scanned the mesocyclone level for all three tornadoes, with heights AGL between 1.41 and 1.85 km for the two
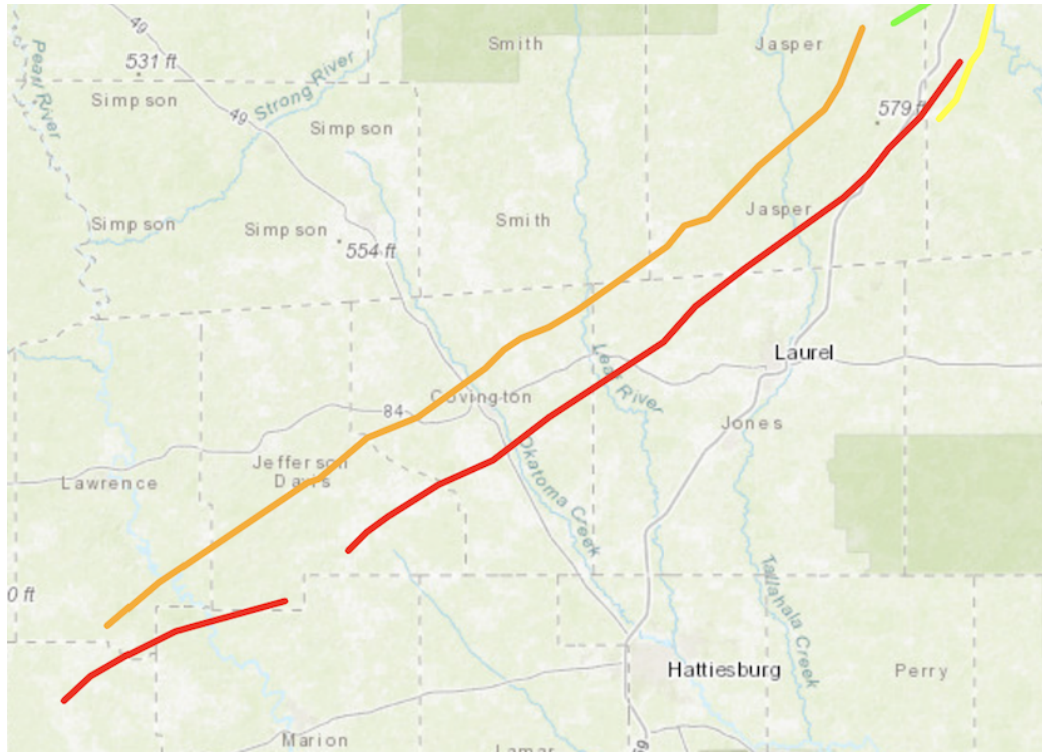
FIG. 3. Tornado tracks for the Walthall and Bassfield EF-4 tornadoes (shown in red) and the Oak Vale EF-3 tornado (shown in orange), 12 April 2020. Credit: NWS Birmingham

EF-4s and between 1.19 km and 1.68 km for the Oak Vale tornado. The maximum Rotation Track values for the Walthall/Bassfield and Oak Vale tornadoes were 0.057 s^{-1} and 0.042 s^{-1}, respectively.

Data from the Walthall/Bassfield and Oak Vale tornadoes differ from the other tornado cases in that at the time of the event, KDGX was running a 0.3° elevation scan with SAILS. In this case, SAILS mode was not running on the 0.5° scan, so 0.5° ΔV updates occurred approximately every 6 mins.

Around the same time, two tornadoes in Alabama, the Millers Hollow EF-1 and Reece City EF-2, formed within one minute of one another (Fig. 4). The Millers Hollow EF-1 tornado travelled a path length of 8.88 km from 23:08 to 23:13 UTC (6:08 PM to 6:13 PM CDT), with no reported injuries or deaths. The Reece City EF-2 tornado travelled a path length of 19.62 km from 23:14 to 23:28 UTC (6:14 PM to 6:28 PM CDT), with no reported injuries or deaths. The end of the Millers Hollow tornado and the beginning of the Reece City tornado damage paths are separated by a 300-400 m increase in terrain height. Ground elevation along the tornado tracks is approximately 600-700 m, with a 1000-m tall ridge between the two tornadoes, with the Millers Hollow tornado to the north of the ridge and the Reece City tornado to the south. NWS Birmingham confirmed these were two separate tornadoes, suggesting it may have been a cyclic tornado event. It is also possible that the ridge caused

a discontinuity in the tornado track without a traditional occlusion of the mesocyclone, but we are unable to confirm this through radar analysis. Recently, simulations by Satrio et al. (2020) found that large terrain features can be disruptive to tornadoes.

For these analyses, the two tornadoes will be referred to collectively as the Reece City tornado in figures and analyses. These two tornadoes were located approximately to the SSE of the Huntsville, AL NEXRAD radar (KHTX). Distance from KHTX for both tornadoes ranged from 85 km to 104 km, and azimuth (direction) around KHTX spanned from 165° (SSE) to 185° (SSW). The radar beam scanned the mesocyclone level with heights between 1.74 km to 2.12 km AGL. The maximum Rotation Tracks value for the two tornadoes was 0.012 s^{-1}.

Several hours later, the Chattanooga EF-3 tornado formed in Tennessee. The Chattanooga tornado travelled a path length of 32.19 km from 03:15 to 03:33 UTC (11:15 PM to 11:33 PM EDT), injuring 19 and killing 3 people. The tornado's distance from KHTX ranged from 73 km to 96 km, and azimuth (direction) from KHTX spanned from 75° (ENE) to 88° (ENE). The radar beam scanned the mesocyclone level with heights between 1.56 km to 1.97 km AGL. The maximum Rotation Tracks value for the Chattanooga tornado was 0.037 s^{-1}.
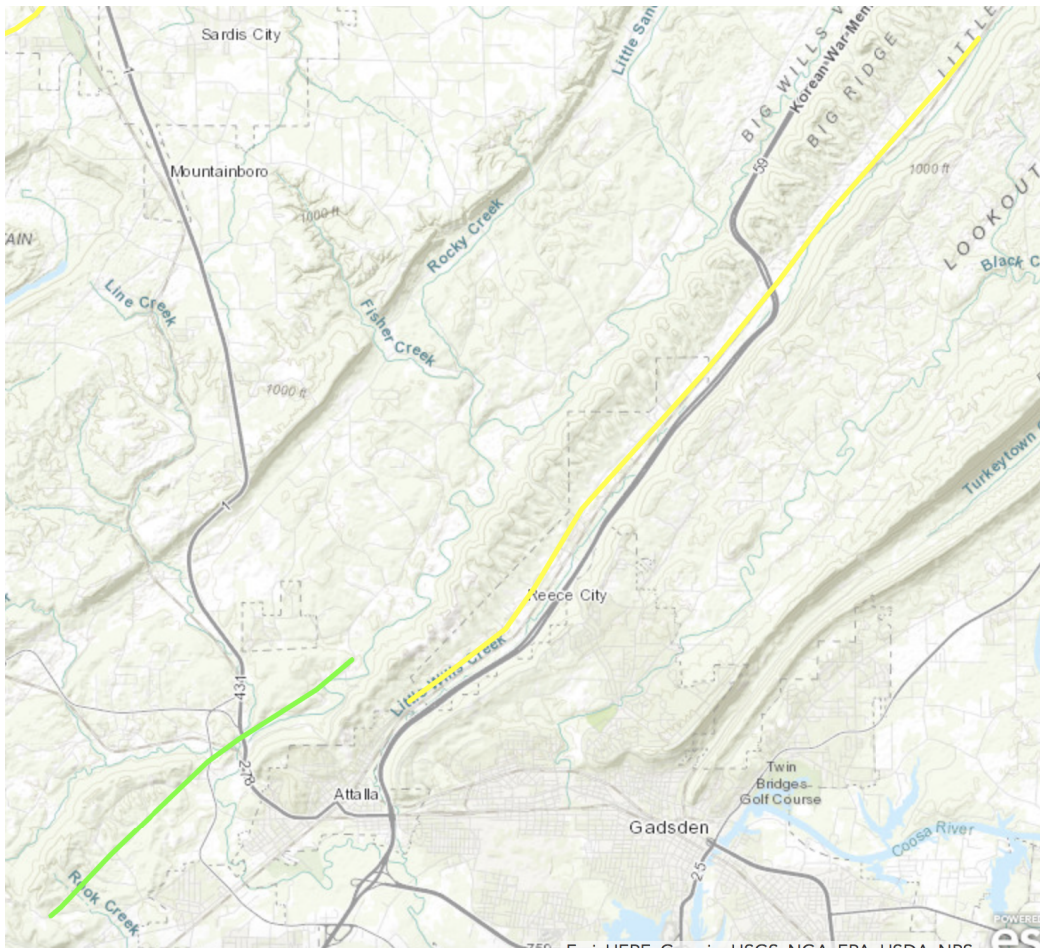
FIG. 4. Tornado tracks for the Millers Hollow EF-1 (shown in green) and the Reece City EF-2 (shown in yellow), 12 April 2020. A ridge separates the two tornado tracks, which the tornadoes follow nearly parallel to. Credit: NWS Birmingham

4. Results

This study investigates several tornado events and examines the relationships between six different variables: ΔV, damage width, maximum EF rating, terrain height, velocity couplet width, and maximum Rotation Tracks (Fig. 5). Analysis is conducted on the $0.5°$ elevation scan data. The velocity couplet width is a measure of the distance between the maximum inbound and outbound velocities in ΔV. Some data points, particularly near the end of the tornado tracks, indicate couplet widths around 10 km, which is larger than a velocity couplet is usually defined by. Thus, note in those instances, the term "couplet" is being used more loosely. Relationships among these variables are determined by calculation of the correlation coefficient (CC; Table 1). To classify the strength of the correlations, CCs are broken into three categories based on the magnitude: weak ($|CC| \leq 0.3$), moderate ($0.3 < |CC| < 0.7$), and strong ($|CC| \geq 0.7$).

a. Nashville Tornado

Prior to tornadogenesis, an area of considerable terrain height variations was present. While it may be a coincidence, it is worthwhile to note that the Nashville tornado began its track after descending from this hilly area. The Nashville tornado is the only event examined in this study that the radar beam scanned below 1 km AGL and thus viewed the tornado-level winds. However, the variables still showed only weak CCs when compared to terrain, with the highest correlation between ΔV and terrain height (CC = 0.259; Fig. 5e). The damage and intensity variables showed several strong correlations in this case. Some of the strongest correlations are between damage width and ΔV (CC = 0.909; Fig. 5a), couplet width and ΔV (CC = -0.874; Fig. 5c), and maximum EF rating and ΔV (CC = 0.722). These values indicate that when ΔV increases, damage width and maximum EF rating also increase, but couplet width decreases. The inverse relationship between ΔV and couplet width relates well to the concept of angular momentum conservation, where a tighter couplet tends to have stronger rotational intensity.
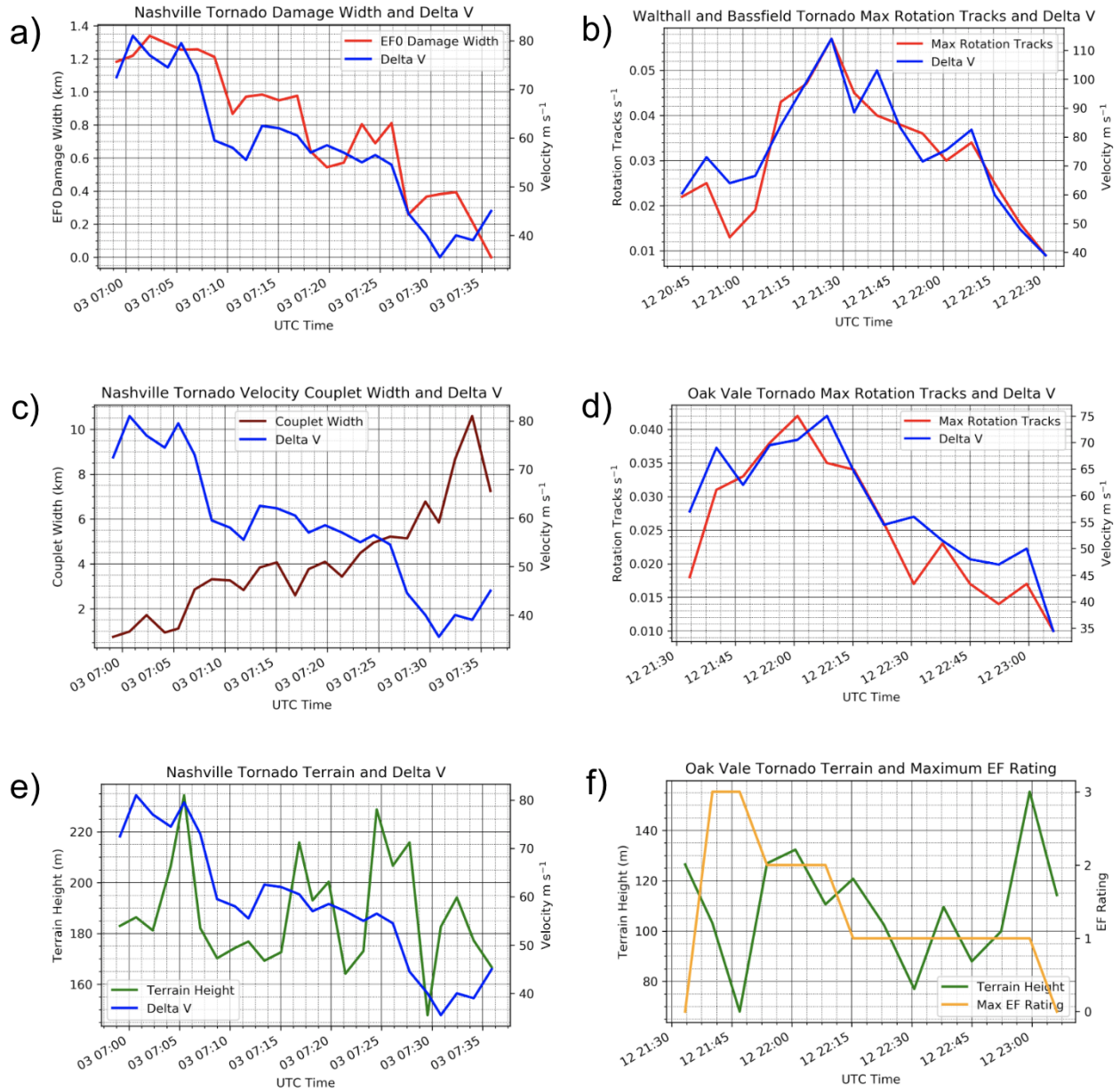
FIG. 5. Plots of variables from the Nashville (a, c, e), Walthall/Bassfield (b), and Oak Vale (d, f) tornadoes. The Nashville tornado showed a strong positive correlation between damage width and ΔV (a) and a strong negative correlation between couplet width and ΔV (c). Strong correlations between maximum Rotation Tracks and ΔV are shown for the Walthall/Bassfield tornadoes (b) and for the Oak Vale tornado (d). Examples of weak terrain correlations are shown for the Nashville tornado between terrain height and ΔV (e) and for the Oak Vale tornado between terrain and maximum EF rating (f).

	NASHVILLE	COOKEVILLE	WALTHALL/ BASSFIELD	OAK VALE	REECE CITY	CHATTANOOGA
Damage Width and Max EF	0.666	0.895	0.610	0.594	0.454	0.830
Damage Width and Delta V	0.909	0.249	0.504	0.608	0.560	0.669
Terrain and Delta V	0.259	-0.685	-0.026	0.076	-0.523	0.364
Terrain and Max EF	-0.005	0.205	0.074	-0.278	0.227	-0.170
Terrain and Damage Width	0.091	0.150	-0.208	-0.234	-0.251	0.116
Max EF and Delta V	0.722	0.113	0.699	0.709	-0.047	0.626
Couplet Width and Delta V	-0.874	0.468	-0.098	-0.617	0.199	-0.332
Terrain and Couplet Width	-0.186	-0.513	-0.523	0.095	0.145	-0.013
Delta V and Max RT	0.680	0.739	0.923	0.904	0.051	0.397
Terrain and Max RT	-0.009	-0.650	0.254	0.110	-0.390	0.310
Max EF and Max RT	0.492	-0.287	0.674	0.723	0.314	0.293
Damage Width and Max RT	0.726	-0.310	0.460	0.600	0.104	0.398
Couplet Width and Max RT	-0.730	0.628	-0.297	-0.610	-0.034	-0.222
Damage and Couplet Width	-0.843	-0.433	-0.056	-0.394	-0.115	-0.689
Couplet Width and Max EF	-0.667	-0.576	-0.254	-0.460	0.286	-0.382

TABLE 1. Calculated correlation coefficients (CCs) between intensity, damage, and terrain variables for each tornado event. Variables include damage width, Delta V (ΔV), maximum EF rating (Max EF), maximum Rotation Tracks (Max RT), terrain height, and couplet width.

Along with the previously mentioned ΔV correlation, there are a few additional strong to high moderate negative correlations between couplet width and other variables, including damage width (CC = -0.843), max Rotation Tracks (CC = -0.730), and maximum EF rating (CC = -0.667). These stronger negative correlations indicate a relationship that when the couplet width is smaller, the intensity and damage severity of the tornado are greater. However, note that by the end of the Nashville track, the tornado was further from KOHX, and the radar beam scanned higher. As the tornado moved away from the radar, both ΔV and couplet width represent the wind profile at a higher altitude than at the beginning of the data set.

b. Cookeville Tornado

Cookeville tornadogenesis began after descending from an area of varying terrain height, and the tornado travelled through a flatter terrain region, comparable to the Nashville tornado. At a further range from KOHX than the Nashville tornado, the radar beam scanned above 1 km for the Cookeville tornado. Thus, for Cookeville, the ΔV calculations are representative of the mesocyclone-level winds. In contrast to the Nashville tornado, the Cookeville tornado was a short-lived event, only lasting about 8 minutes. The SAILS scans allowed 0.5° updates approximately every 1.5 minutes. With this short of a lifetime and the limitation of time gaps in radar scanning, the number of available data points is sparse.

Strong CCs exist between variables, including damage width and maximum EF rating (CC = 0.895) and also ΔV and maximum Rotation Tracks (CC = 0.739). Terrain correlations also indicate moderate CCs with ΔV (CC = -0.685), maximum Rotation Tracks (CC = -0.650), and

couplet width (CC = -0.513). In addition, CCs between the maximum EF rating and other variables for Cookeville indicate different relationships than in the other tornado cases. Maximum EF rating shows a weak correlation with ΔV (CC = 0.113) and a negative correlation with maximum Rotation Tracks (CC = -0.287), both of which differ from other cases.

c. Walthall/Bassfield and Oak Vale Tornadoes

Since the 0.5° velocity scan for KDGX updated every 6 mins, all variables for this case were also recorded at the same time steps. The Walthall/Bassfield (W/B) and Oak Vale (OV) CCs show very similar characteristics between these tornado events. While the tornadoes formed from two different supercells, the tornado tracks were separated spatially by only around 16 km. Recall that the Bassfield damage width data is recorded for the EF-1 contour as opposed to the EF-0 contour. In general, CCs for both events indicate the same correlation strengths between variables. Note that for these cases ΔV is measured from the mesocyclone level. The strongest correlations are found between ΔV and maximum Rotation Tracks (W/B CC = 0.923; OV CC = 0.904; Fig. 5b, d), maximum EF rating and maximum Rotation Tracks (W/B CC = 0.674; OV CC = 0.723), and maximum EF rating and ΔV (W/B CC = 0.699; OV CC = 0.709). In these cases, ΔV and maximum Rotation Tracks are highly correlated because both variables are representative measurements of the mesocyclone-level winds. However, the couplet width correlations between the two events are not similar for ΔV (W/B CC = -0.098; OV CC = -0.617) and for terrain height (W/B CC = -0.523; OV CC = 0.095), with one with a moderate CC and the other with a weak CC. Terrain correlations remain low with a single moderate value for couplet width (W/B CC

= -0.523), and the next highest being only a weak correlation between terrain and maximum EF rating (OV CC = -0.278; Fig. 5f).

d. Reece City Tornadoes

The Reece City event shows relatively weaker correlations compared to the other cases, with the highest being a moderate CC between damage width and ΔV (CC = 0.560). The most significantly different correlation from the other cases is between ΔV and maximum EF rating, with a very low and negative value (CC = -0.047). Note that the radar data for ΔV represents mesocyclone-level winds, with some measurements taken at a beam height of greater than 2 km AGL. These two tornadoes are also the weakest on the EF-scale examined in this study, with an EF-1 and EF-2.

e. Chattanooga Tornado

Similarly, the Chattanooga tornado provides another example of mesocyclone-level winds, having beam heights slightly below 2 km. CCs in this event indicate damage and intensity variables are well correlated, with the highest between damage width and maximum EF rating (CC = 0.830), damage width and ΔV (CC = 0.669), and maximum EF rating and ΔV (CC = 0.626). However, terrain correlations still remain low to moderate, with the strongest correlation between terrain and ΔV (CC = 0.364).

5. Synthesis

The Nashville and Cookeville tornadoes offer unique perspectives of similar strength tornadoes with different radar signatures and tornadogenesis locations descending from hilly areas. While the Nashville tornado dissipated when it ascended into another hilly area, the Cookeville tornado dissipated in a region without significant terrain variation. Though the Nashville tornado (63 mins) lasted longer than the Cookeville tornado (8 mins), the Nashville tornado showed slightly less peak damage severity, rated as an EF-3 versus the Cookeville EF-4. However, the velocity signature of the Cookeville tornado on radar appeared weaker than the Nashville tornado. The Nashville tornado travelled closer to the radar, with its nearest point only about 9 km south of KOHX (Fig. 6). It moved toward the east away from the radar site. Since the Cookeville tornado touched down shortly after the Nashville tornado had dissipated from the same supercell that continued to travel away from KOHX, the range from KOHX for the Cookeville tornado was much greater than for the Nashville tornado. With a greater range, the radar beam was higher AGL when it scanned the Cookeville tornado velocities, and the spatial resolution was reduced due to beam broadening. Thus, the radar Doppler velocity
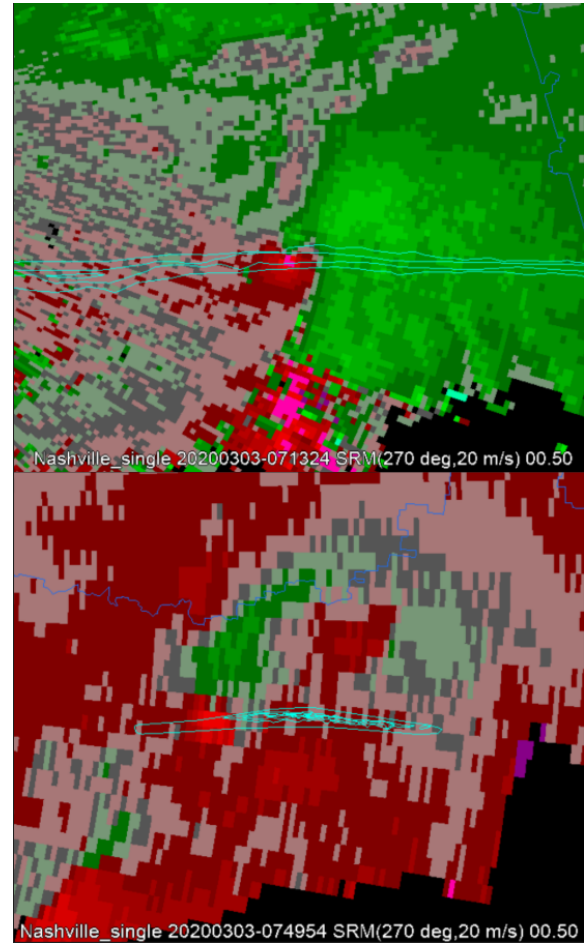

FIG. 6. KOHX PPI scans from the WDSS-II display of 0.5° storm-relative Doppler velocity from the Nashville tornado (top) and Cookeville tornado (bottom), 3 March 2020.
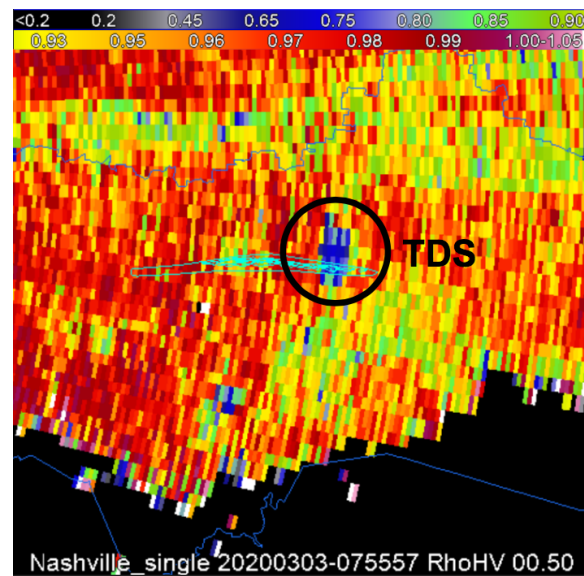

FIG. 7. KOHX PPI scan from the WDSS-II display of 0.5° cross-correlation coefficient (ρ_{hv}) from the Cookeville tornado, showing a strong tornadic debris signature (TDS), 3 March 2020.

Terrain Correlations			
	WEAK	MODERATE	STRONG
Delta V	3	3	0
Damage Width	6	0	0
Max EF Rating	6	0	0
Max RT	3	3	0
Couplet Width	4	2	0

TABLE 2. Terrain correlation strengths for each tornado event (out of 6) with the five other variables are shown. Categories are based on the magnitude CCs into weak ($|CC| \leq 0.3$), moderate ($0.3 < |CC| < 0.7$), and strong ($|CC| \geq 0.7$).

ΔV Correlations			
	WEAK	MODERATE	STRONG
Terrain	3	3	0
Damage Width	1	4	1
Max EF Rating	2	2	2
Max RT	1	2	3
Couplet Width	2	3	1

TABLE 3. Same as Table 2, but instead showing variable correlations with ΔV.

Damage Width Correlations			
	WEAK	MODERATE	STRONG
Terrain	6	0	0
Delta V	1	4	1
Max EF Rating	0	4	2
Max RT	1	4	1
Couplet Width	2	3	1

TABLE 4. Same as Table 2, but instead showing variable correlations with damage width.

showed mesocyclone-level winds for the Cookeville tornado rather than the strong low-level tornado winds, as in the Nashville tornado (Fig. 6). Even though the Cookeville tornado velocity signature appeared weaker, correlation coefficient (ρ_{hv}) scans indicated a strong TDS associated with the tornado (Fig. 7).

To compare the six tornado events, correlations with terrain height, ΔV, and damage width are categorized based on strength. Most of the correlations with terrain height (73%) fit into the weak correlation category (Table 2). Terrain correlations with damage width and maximum EF rating show weak CCs in all six cases. Few variables indicate a moderate correlation (27%) to terrain, including ΔV, maximum Rotation Tracks, and couplet width. The moderate terrain and ΔV correlations do not include the Nashville tornado, so they only include cases in which ΔV represented the mesocyclone-level winds. None of the variables show a strong correlation with terrain. We do note, however, that the tornadogenesis locations occurred across a large gradient in elevation and elevation variability for at least two tornado events.

Correlations with ΔV (Table 3) indicate a higher number of cases in the strong (23%) and moderate (47%) cat-

egories compared to the terrain height correlations. Weak correlations only account for less than one-third (30%) of the total correlations with ΔV. Maximum Rotation Tracks shows the best overall correlation with ΔV in the six tornado cases, with three categorized as strong and two categorized as moderate. Maximum EF rating shows an even split between the cases, with two in each correlation strength category. Interestingly, the two weakest correlations with ΔV and maximum EF rating are from the Reece City and Cookeville tornadoes, respectively the weakest and shortest tornado events examined in this study. ΔV correlations with damage width and couplet width indicate only one tornado event in each, and both of these strong values are from the Nashville. The Nashville tornado ΔV showed a strong positive correlation to damage width and a strong negative correlation to couplet width. Note again that Nashville was the only case in this study in which the tornado-level winds were examined by the radar.

Correlations with damage width (Table 4) show a smaller number of strong cases (17%). As previously mentioned, terrain shows only weak correlations with damage width. Without including the terrain correlations, the majority of damage width correlations fall into the moderate category (63%). Damage width correlations with maximum EF rating show no cases in the weak category, all of which are positive correlations, suggesting a general trend that higher rated tornadoes are accompanied by wider damage tracks. The two strong maximum EF rating and damage width correlations are from the Cookeville and Chattanooga cases, both of which are relatively shorter yet stronger events. The single strong correlations in ΔV, maximum Rotation Tracks, and couplet width with damage width are all from the Nashville case, with the couplet width correlation being strongly negative.

6. Conclusion

This study explored the correlations among radar velocities, terrain height, and surface damage for eight tornadoes, analyzed in six cases. In general, the stronger tornadoes in the study (EF-3 and EF-4) tend to show that ΔV and maximum EF rating are well correlated. The Cookeville case proved to be an exception to this with a weaker correlation in these variables due to the small diameter and short duration of the event. On another note, the Nashville tornado, which is the only case in the study that the data represented tornado-level winds, showed very little correlation to terrain. While it was the closest example of winds near the ground, terrain still seemed to not be a very important factor in the Nashville tornado event, or at least terrain effects were not evident on the temporal and spatial scales resolvable by NEXRAD.

While it is outside the scope of this study, the Nashville and Cookeville tornado events showed interesting changes in terrain features outside of the tornado tracks. Before

the start and at the end of the Nashville track, regions of significant variations in terrain height lie on either side. On the other side of the complex terrain following the Nashville tornado, the Cookeville tornado started on the other side of the hilly region. Both of these tornadoes show little significant variation in terrain along the tracks. This study focused only on data along the damage tracks of tornadoes, but it is interesting to note the areas of varying terrain height on either side of the track where tornadogenesis and tornado dissipation occur and merits further investigation.

While some general observations are noted, data limitations, especially with the NEXRAD radar data, make establishing trends more challenging. SAILS allowed for more rapid updates in velocity data collection in the 0.5° elevation scan, which was the main level this study examined. However, with the Walthall/Bassfield and Oak Vale tornadoes, SAILS were not used on the 0.5° scan, so velocity data updates were spaced out by about three times as long as the other cases. Both of these events lasted longer amounts of time, so the data sample still included a useful number of points. Additionally, NEXRAD radars are limited by the range to the target and beam height, which is a function of the range. Though each case utilized the 0.5° elevation scan, differences in distance from the radar to the target changed the level at which the velocity data was recorded. At a close range to the radar, such as in the Nashville case, low-level tornado winds were recorded. In all the other cases, in which the tornadoes occurred farther away from the radar, velocity data above 1 km was recorded, and thus representative of the mesocyclone-level winds. These limitations of the NEXRAD system produce difficulty in determining trends based on the cases in this study because of differences in levels scanned and number of collected data points.

Because of the limitations with the NEXRAD system, it would be beneficial in a future study to use rapid-scan radar data (Pazmany et al. 2013; Isom et al. 2013; Kurdzo et al. 2017) to analyze correlations among tornado intensity, damage, and terrain. Rapid-scan radars would allow data collection at more levels in quicker time, so it could record even quick changes in tornado structure and intensity that the NEXRAD radars are unable to resolve. When looking at terrain impacts on tornadoes, rapidly updating data is necessary because of quick tornado translation speeds over abrupt changes in terrain height. Slower updating radar data with NEXRAD radars make seeing any smaller terrain-induced changes difficult. The use of rapid-scan radars in a future study would record more data in both the tornado-level and mesocyclone-level winds and further explore terrain impacts on these circulations.

References

Bodine, D., M. R. Kumjian, R. D. Palmer, P. L. Heinselman, and A. V. Ryzhkov, 2013: Tornado Damage Estimation Using Polarimetric Radar. *Wea. Forecasting*, **28**, 139–158, doi:10.1175/WAF-D-11-00158.1.

Brooks, H. E., and J. Correia, James, 2018: Long-Term Performance Metrics for National Weather Service Tornado Warnings. *Weather and Forecasting*, **33 (6)**, 1501–1511, doi:10.1175/WAF-D-18-0120.1.

Brown, M. C., and C. J. Nowotarski, 2020: Southeastern U.S. Tornado Outbreak Likelihood Using Daily Climate Indices. *Journal of Climate*, **33 (8)**, 3229–3252, doi:10.1175/JCLI-D-19-0684.1.

Brown, R. A., L. R. Lemon, and D. W. Burgess, 1978: Tornado Detection by Pulsed Doppler Radar. *Monthly Weather Review*, **106 (1)**, 29–38, doi:10.1175/1520-0493(1978)106⟨0029:TDBPDR⟩2.0.CO;2.

Chrisman, J. N., 2013a: Dynamic Scanning. *Radar Operations Center NEXRAD Now*, **22 (1-3)**, URL http://www.roc.noaa.gov/WSR88D/PublicDocs/NNOW/NNow22c.pdf.

Crum, T. D., R. E. Saffle, and J. W. Wilson, 1998: An Update on the NEXRAD Program and Future WSR-88D Support to Operations. *Weather and Forecasting*, **13 (2)**, 253–262, doi:10.1175/1520-0434(1998)013⟨0253:AUOTNP⟩2.0.CO;2.

Godfrey, C. M., and C. J. Peterson, 2017: Estimating Enhanced Fujita Scale Levels Based on Forest Damage Severity. *Weather and Forecasting*, **32 (1)**, 243–252, doi:10.1175/WAF-D-16-0104.1.

Isom, B., and Coauthors, 2013: The Atmospheric Imaging Radar: Simultaneous Volumetric Observations Using a Phased Array Weather Radar. *J. Atmos. Oceanic Technol.*, **30**, 655 – 675, doi:10.1175/JTECH-D-12-00063.1.

Karstens, C. D., J. Gallus, William A., B. D. Lee, and C. A. Finley, 2013: Analysis of Tornado-Induced Tree Fall Using Aerial Photography from the Joplin, Missouri, and Tuscaloosa–Birmingham, Alabama, Tornadoes of 2011*. *Journal of Applied Meteorology and Climatology*, **52 (5)**, 1049–1068, doi:10.1175/JAMC-D-12-0206.1.

Kurdzo, J. M., and Coauthors, 2017: Observations of Severe Local Storms and Tornadoes with the Atmospheric Imaging Radar. *Bull. Amer. Meteor. Soc.*, **98**, 915 – 935, doi:10.1175/BAMS-D-15-00266.1.

Lakshmanan, V., T. Smith, G. Stumpf, and K. Hondl, 2007: The Warning Decision Support System–Integrated Information. *Weather and Forecasting*, **22 (3)**, 596–612, doi:10.1175/WAF1009.1.

Lewellen, D. C., 2012: 4B. 1 Effects of Topography on Tornado Dynamics: A Simulation Study. 26th Conference on Severe Local Storms (5 - 8 November 2012) Nashville, TN, American

Meteorological Society. URL https://ams.confex.com/ams/26SLS/webprogram/Paper211460.html.

Mahalik, M. C., B. R. Smith, K. L. Elmore, D. M. Kingfield, K. L. Ortega, and T. M. Smith, 2019: Estimates of Gradients in Radar Moments Using a Linear Least Squares Derivative Technique. *Weather and Forecasting*, **34 (2)**, 415–434, doi:10.1175/WAF-D-18-0095.1.

Markowski, P. M., and N. Dotzek, 2011: A Numerical Study of the Effects of Orography on Supercells. *Atmospheric Research*, **100 (4)**, 457–478.

Miller, M. L., V. Lakshmanan, and T. M. Smith, 2013: An Automated Method for Depicting Mesocyclone Paths and Intensities. *Weather and Forecasting*, **28 (3)**, 570–585, doi:10.1175/WAF-D-12-00065.1.

Mitchell, E. D. W., S. V. Vasiloff, G. J. Stumpf, A. Witt, M. D. Eilts, J. T. Johnson, and K. W. Thomas, 1998: The National Severe Storms Laboratory Tornado Detection Algorithm. *Weather and Forecasting*, **13 (2)**, 352–366, doi:10.1175/1520-0434(1998)013⟨0352:TNSSLT⟩2.0.CO;2.

Oswalt, S. N., W. B. Smith, P. D. Miles, and S. A. Pugh, 2014: Forest Resources of the United States, 2012: A Technical Document Supporting the Forest Service 2010 Update of the RPA Assessment. *Gen. Tech. Rep. WO-91. Washington, DC: US Department of Agriculture, Forest Service, Washington Office. 218 p.*, **91**.

Pazmany, A. L., J. B. Mead, H. B. Bluestein, J. C. Snyder, and J. B. Houser, 2013: A Mobile Rapid-Scanning X-band Polarimetric (RaXPol) Doppler Radar System. *J. Atmos. Oceanic Technol.*, **30 (7)**, 1398–1413, doi:10.

Ryzhkov, A. V., T. J. Schuur, D. W. Burgess, and D. S. Zrnic, 2005: Polarimetric Tornado Detection. *J. Appl. Meteor.*, **44**, 557–570, doi:10.1175/JAM2235.1.

Satrio, M. A., D. J. Bodine, A. E. Reinhart, T. Maruyama, and F. T. Lombardo, 2020: Understanding How Complex Terrain Impacts Tornado Dynamics Using a Suite of High-Resolution Numerical Simulations. *J. Atmos. Sci*, accepted.

Smith, B. T., R. L. Thompson, A. R. Dean, and P. T. Marsh, 2015: Diagnosing the Conditional Probability of Tornado Damage Rating Using Environmental and Radar Attributes. *Weather and Forecasting*, **30 (4)**, 914–932, doi:10.1175/WAF-D-14-00122.1.

Smith, T. M., and Coauthors, 2016: Multi-Radar Multi-Sensor (MRMS) Severe Weather and Aviation Products: Initial Operating Capabilities. *Bulletin of the American Meteorological Society*, **97 (9)**, 1617–1630, doi:10.1175/BAMS-D-14-00173.1.

Thompson, R. L., and Coauthors, 2017: Tornado Damage Rating Probabilities Derived from WSR-88D Data. *Weather and Forecasting*, **32 (4)**, 1509–1528, doi:10.1175/WAF-D-17-0004.1.

WSEC, 2006: A Recommendation for an Enhanced Fujita Scale (EF-scale), Revision 2. Wind Science and Engineering Center Rep., Texas Tech University, Lubbock, TX, 95 pp. URL http://www.depts.ttu.edu/nwi/pubs/fscale/efscale.pdf.